

Multimodal Distributions along the Horizontal Branch ¹

Francesco R. Ferraro², Barbara Paltrinieri², Flavio Fusi Pecci^{2,3}

Ben Dorman^{4,5} and Robert T. Rood⁴

ABSTRACT

We report on HST/WFPC2 *U*, *V* and far-ultraviolet observations of two Galactic Globular Clusters (GGCs), NGC 6205 = M13 and NGC 6093 = M80. Both of these clusters have horizontal-branch (HB) tails that extend to the helium-burning main sequence, with the hottest stars reaching theoretical effective temperatures above 35,000 K. In both clusters, groups of stars are found to be separated by narrow gaps along the blue HB sequence. These gaps appear at similar locations in the color-magnitude diagrams of the two clusters. While stochastic effects may give rise to variations in the color distribution along the HB, the coincidence of gaps in different clusters effectively rules this out as the primary cause. The comparison among the clusters strongly suggests that there are separate physical processes operating during the earlier red-giant phase of evolution to produce mass loss.

Subject headings: globular clusters: individual (M80, M13, M3)—stars: horizontal-branch—ultraviolet: stars—stars: evolution

¹Based on observations with the NASA/ESA *Hubble Space Telescope*, obtained at the Space Telescope Science Institute, which is operated by AURA, Inc., under NASA contract NAS5-26555

²Osservatorio Astronomico di Bologna, via Zamboni 33, I-40126 Bologna, ITALY

³Stazione Astronomica di Cagliari, 09012 Capoterra, ITALY

⁴Astronomy Dept, University of Virginia, P.O.Box 3818, Charlottesville, VA 22903-0818

⁵Laboratory for Astronomy & Solar Physics, Code 681, NASA/GSFC, Greenbelt MD 20771

1. Introduction

A growing number of Galactic Globular Clusters (GGCs) have been found to show discontinuous stellar distributions along the horizontal-branch (HB). Some of them are clearly bimodal with a HB clump of red stars and a tail of blue, hot stars populating the blue side of the RR Lyrae strip (NGC 2808—Ferraro et al. 1990; NGC 1851—Walker 1992; NGC 6229—Borissova et al. 1997) and more recently NGC 362 (Dorman et al. 1997a), NGC 6388 and NGC 6441 (Rich et al. 1997). In other clusters the stellar distribution in the HB blue tails (BTs) is interrupted by underpopulated regions or “gaps” (see for example NGC 6752—Buonanno et al. 1986; M15—Buonanno, Corsi, & Fusi Pecci 1985). NGC 2808 (Sosin et al. 1997) shows both phenomena: it has both a red clump and an extended blue sequence with three groups separated by narrow gaps.

The maximum possible extent of the HB tail is ~ 4.5 mag where it reaches the He-burning main sequence. This limit is reached in a number of clusters, including NGC 6752, NGC 2808, ω Cen and the subjects of this paper, M13 and M80. These extreme blue tail (EBT) clusters form an important subclass of BT clusters. All clusters found to date with EBTs have indistinguishable $[\text{Fe}/\text{H}]$, close to -1.5 . However, not all BT clusters with this metallicity have EBTs. For example, M79 has a BT which extends 3 mag below the level of the HB but still falls far short of the He-burning main sequence (Hill et al. 1996). The bluest stars in EBTs are often separated from their slightly cooler counterparts by a gap analogous to that seen for the subdwarf B stars in the Galactic field.

The distribution in color along the HB is understood to be due to a distribution in the envelope masses of stars leaving the red-giant branch (RGB; see Rood 1973, Buonanno et al. 1985, Fusi Pecci et al. 1993). Clusters with extended blue HB sequences often show gaps whose physical origin is still a mystery. They cannot be produced by standard single population HB simulations except as statistical artefacts (Crocker, Rood, & O’Connell 1988, Catelan et al. 1997, but see also the claims by Lee, Demarque and Zinn 1994). If gaps are observed at the same location in more than one cluster HB sequence, then statistical fluctuation is unlikely to be the cause. The reality and origin of gaps has been the subject of several studies (Rood & Crocker 1985, Buonanno, Corsi, & Fusi Pecci 1985, Crocker, Rood, & O’Connell 1988,

Bailyn et al. 1992, Catelan et al. 1997).

It is important to bear in mind, though, that even though gaps in cluster HBs may be most apparent in the clusters at metallicity $[\text{Fe}/\text{H}] = -1.5$, but their causes may still be active in clusters at different abundances. In metal-rich clusters, the HBs are collapsed to the red, and gaps that might be present are obscured. In the most metal-poor regime, the sensitivity of a star’s initial position on the ZAHB to envelope mass ($d \log T_{\text{eff}}/dM_{\text{env}}$) is reduced. A gap in mass δM_{env} that produces a gap at $[\text{Fe}/\text{H}] = -1.5$ would not necessarily produce a gap at $[\text{Fe}/\text{H}] = -2.3$. Instead, a dip in the stellar density might result as suggested for M92 by Crocker et al. (1988).

Apart from age variations (see the discussion in the review by Stetson et al. 1996), theoretical studies of HB morphology all require assumptions about the amount and distribution of mass loss on the RGB. Unfortunately, the precise understanding of mass loss from cool stars is one of the most vexing problems in stellar evolution theory. Indeed, the basic underlying mechanism(s) for mass loss has (have) not been firmly identified. Here, we adopt as a working hypothesis that *there is a relationship between gaps and mass loss*. This suggests that either there is more than one mass loss mechanism or that a single mechanism can lead to a multiplicity of results. By adopting this hypothesis, we hope to advance our understanding of both phenomena.

There are some indications that the structural parameters of the parent cluster (see Fusi Pecci et al. 1993, Fusi Pecci 1996, Buonanno et al. 1997) or stellar rotation (Renzini 1977, Fusi Pecci & Renzini 1978, Peterson, Rood, & Crocker 1995) might play a role in HB morphology. Both could plausibly affect mass loss directly. In addition, both might lead to mixing phenomena occurring on the RGB (see Sweigart 1997). Multimodal HBs could easily arise: additional mass loss occurs if the rotation rate exceeds some critical value; a star visits the cluster center or not while on the upper RGB; a star mixes or not. Because these and other candidate processes are difficult or impossible to model from first principles, a first crucial step in understanding is to secure data for and make comparisons between clusters. When do gaps occur? What are the physical parameters (T_{eff} , $\log g$) of the gaps? Comparisons must be made to explore the different dimensions of parameter space, e.g., central cluster density at fixed abundance; abundance at fixed density.

In this paper, we consider the HB morphology of three clusters with HB tails of similar metallicity ($[\text{Fe}/\text{H}] \approx -1.5$) but different HB tails. M13 and M80, using data taken from our Cycle 5 HST/WFPC2 program (GO-5903), and M3 from our Cycle 4 HST/WFPC2 program (GO-5420). We study the detailed morphology of the HB sequence in far-UV/ U /optical colors, since in UV CMDs the HB is approximately horizontal even at high T_{eff} . To the extent possible, we make comparisons with gap locations previously observed in other clusters (NGC 2808, NGC 6752, NGC 6681, ω Cen).

2. Results

Exposures for M80 and M13 were taken through the U , B , V (= F336W, F439W, F555W) and the mid- and far-UV filters (F255W, F160BW) mapping the cluster cores. Here we use only U , V , far-UV exposures. The CMDs presented here are *preliminary results* of the four WFPC2 fields obtained with the the PC located on the cluster center. The detailed description of the exposures and data reduction procedure will be given elsewhere (see Ferraro et al. 1997a for a brief description). All the instrumental magnitudes have been converted to a fixed aperture and then calibrated to the STMAG system using Table 9 in Holtzman et al (1995).

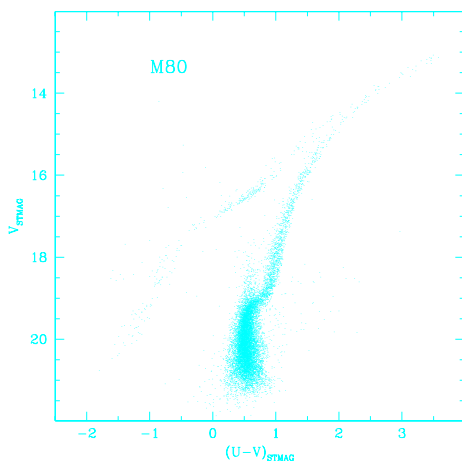


Fig. 1.— The $(V, U - V)$ color magnitude diagram for $\text{NGC}6093 = \text{M80}$.

Figure 1 shows the $(V, U - V)_{\text{STMAG}}$ ⁶ color-magnitude diagram (CMD) for more than 13,000 stars identified in the central region of M80. All the stars found in the PC and WFs cameras are plotted. The reader is referred to Figure 1 of Ferraro et al. (1997b) for the CMDs of M13 and M3.

The most notable features of the M80 CMD are: (1) a very long blue tail of the HB, extending ~ 4.5 mag (just as seen in M13, NGC 6752 and the blue side of NGC 2808); (2) a non-uniform of the stellar distribution along the HB, with at least 4 groups of stars separated by gaps at $V \sim 17.1, 17.5,$ and 18.8 . (3) a relatively large population of supra-HB stars, which will be discussed further in Dorman et al. (1997b); and (4) a large population of blue stragglers, more similar to that found in M3 than to M13 (Ferraro et al. 1997b). We anticipated a substantial UV bright population on the basis of integrated UV colors (van Albada, de Boer, & Dickens 1981, de Boer 1985). The long blue tail of the M80 HB has been previously observed in the deep $(U, U - B)$ CMD of Shara and Drissen (1995). Their HB extension (ranging from $U \sim 17$ down to $U \sim 19$) agrees well with that found from our CMD. However, the four groups of HB stars clearly visible in our Figure 1 can be barely identified in the Shara & Drissen CMD, perhaps due to their use of aperture photometry which typically gives larger errors than PSF fitting.

Recently, the long blue tail of the HB has also been observed in a ground-based study of the outer parts of the cluster (Brocato et al. 1997), but again the gaps are only barely visible in that diagram.

3. The Detailed HB Structure of M3, M13 & M80

The metallicity of M80 is similar to that of M3 and M13. The Zinn (1985) scale gives the metallicities of M3, M13, and M80 respectively as (1986) $[\text{Fe}/\text{H}] = -1.66, -1.64,$ and -1.65 . Note that new high resolution spectra suggest higher $[\text{Fe}/\text{H}]$ values for M3 and M13, $[\text{Fe}/\text{H}] \sim -1.47$ and -1.51 , (Kraft et al. 1992) and $[\text{Fe}/\text{H}] \sim -1.34$ and -1.39 (Carretta and Gratton 1997 [CG97]). We assume that the determination of the abundance differential between the clusters is more robust than the absolute value. Using equation 7 in CG97 to convert the Zinn value to

⁶All magnitudes quoted here are in the STMAG system, i.e. $m_{\lambda} = -2.5 \log F_{\lambda} - 21.1$, where F_{λ} is the flux per unit wavelength received through a filter with effective wavelength λ .

CG97 scale gives $[\text{Fe}/\text{H}] \sim -1.4$ for M80.

To get a better impression of the similarities in the overall morphology in the CMD we align the clusters in the $(V, U - V)_{\text{STMAG}}$ CMD, shifting the CMDs to match the M13 principle sequences and then co-adding the result. The shifts necessary are: $\delta V = -1.3$ and $\delta(U - V) \sim -0.3$ for M80 and $\delta V = -0.6$ and $\delta(U - V) \sim -0.03$ for M3. The color shifts imply $\Delta E(B - V)_{M80-M13} \lesssim 0.15$ and $\Delta E(B - V)_{M3-M13} \lesssim 0.015$ (see Dorman et al. 1997b for further discussion).

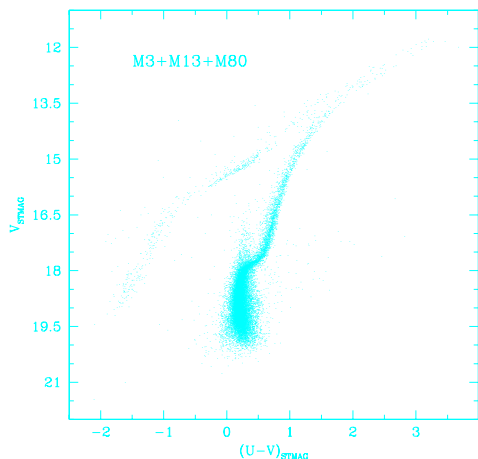


Fig. 2.— The coadded $(V, U - V)$ CMD for M13, M80 and M3. M80 and M3 have been aligned with M13 shifts in $(U - V), V$. See text for details.

Figure 2 shows the combined CMD, in which more than 50,000 stars have been plotted. As can be seen from the small scatter along the RGB and HB the sequences match well, showing the high degree of similarity of the main branches in the CMD for these clusters. Moreover the HB multi-group distribution is still (perhaps more obviously) present. For this to be the case the gaps along the HB of these clusters must have very similar locations in the CMD. In addition, the HB of M3 nicely matches the reddest part of the HB in M13 and M80. Note that in this plane the RR Lyrae gap occurs at $(U - V) \sim 0.55$ and the red HB covers a quite small range in color, since the $(U - V)$ color is quite insensitive to T_{eff} for temperatures less than or equal to those of RR Lyrae stars

(Ferraro et al. 1997b).

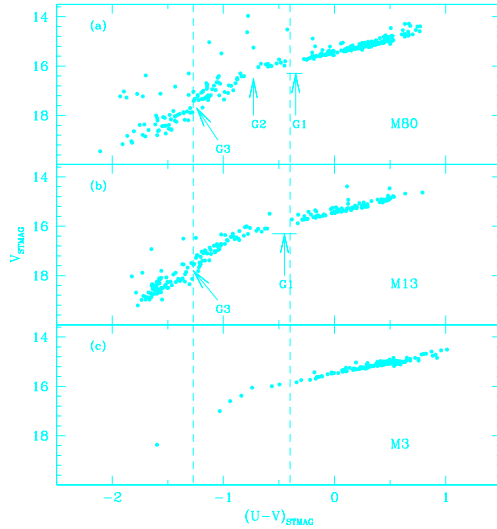


Fig. 3.— The HB in the $(U - V, V)$ plane, for M3, M13 and M80, respectively, after the alignment to M13 (see text). Only non-variable stars have been plotted for M3. Gaps discussed in the text are shown. Note that in this plane the RR Lyrae gap occurs at $(U - V) = 0.55$ and it is not visible in the CMD since it spans a small range in color.

In order to bring out the similarities, we show in Figure 3 a comparison of the HB of each cluster in the $(V, U - V)$ plane after alignment. The relative population of HB stars in the three clusters is 292, 230 and 163 in M80, M13 and M3, respectively (only non-variable stars have been considered). These numbers reflect the larger mass estimated for M80 and the large fraction of M3 stars which is variable.

Figure 4 shows the comparison of the HB of M13 and M80 in the $(m_{160}, m_{160} - V)$ plane. A shift of $\delta m_{160} = -1.95$ and $\delta(m_{160} - V) \sim -0.75$ has been applied to M80 to match the M13 sequence. Figure 5 shows the $U, U - V$ CMD.

The gaps are more obvious in some planes than in others, but each gap we discuss is present in each plane. Several important features can be seen in these figures. First, the location of the cooler gap in M13 and M80, labeled G1, is almost coincident with the blue edge of the bulk of the HB population in M3. Second, the hottest gap is found in similar positions in both M13 and M80. Third, M80 appears to have another gap, G2. In Figure 5 we see that the M80

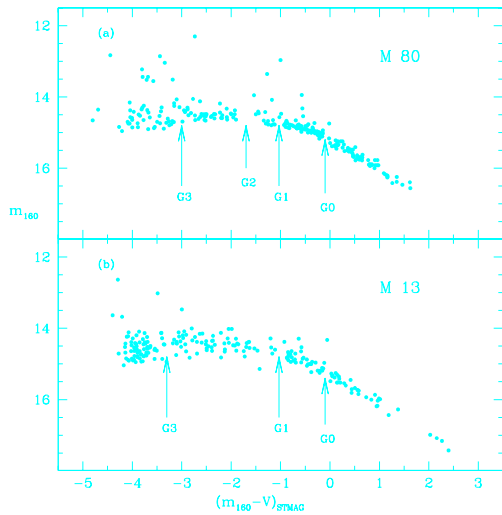


Fig. 4.— The HB in the $(m_{160}, m_{160} - V)$ plane, for M13 and M80, respectively. A shift of $\delta m_{160} = -1.95$ and $\delta(m_{160} - V) \sim -0.75$ has been applied to M80 HB to match M13. Gaps discussed in the text are shown.

stars between G1 and G2 define a sequence somewhat more luminous than that of the adjacent regions or in the comparable part of M13 (see panel c). Finally, Figures 4 and 5 show an additional gap, G0, located at $(m_{160} - V) \sim 0$. G0 is less apparent in the $V, U - V$ CMD because of the compression of the T_{eff} scale in the $U - V$ color. However, careful examination of Figure 3 does reveal features which can be associated with G0.

A preliminary comparison with the theoretical models (Dorman et al. 1993) shows that G1 is located at $T_{\text{eff}} \sim 11,000$ K, G2 at $T_{\text{eff}} \sim 12,000$ K and G3 at $T_{\text{eff}} \sim 19,500$ K in M13 and $T_{\text{eff}} \sim 18,000$ K in M80, and G0 at $T_{\text{eff}} \sim 9,500$ K. It is quite remarkable that G0, G1, and G3 are located at nearly the same temperature (within 1500 K) in each cluster.

4. ℓ_{HB} : A Linear Coordinate along the HB

In order to study the stellar distribution along the HB properly and to test for the existence and significance of features like gaps, Rood & Crocker (1985, hereafter RC85) and Crocker et al. (1988) introduced a coordinate which was “linear” along the entire length of the HB. Such a coordinate was required to avoid “artificial” features (clumps, etc.)

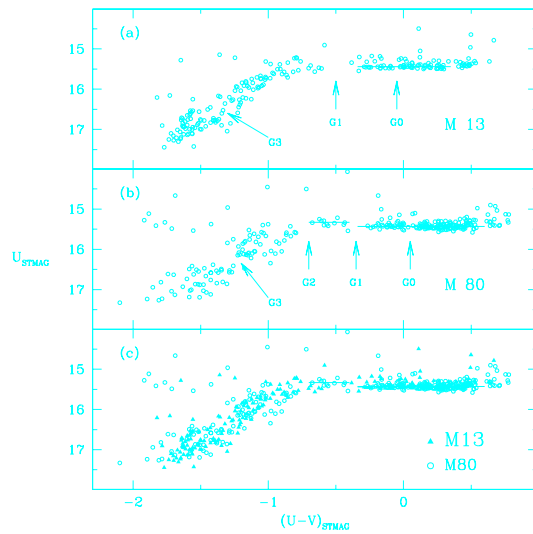


Fig. 5.— The HB in the $(U, U - V)$ plane, for M13 [panel (a)] and M80 [shifted to match M13 panel (b)], respectively. The luminosity of the stars between G1 and G2 (with respect to the “horizontal” region of the HB in this plane) is also shown. In panel (c) the HB stars in M80 (empty circles) from panel (a) have been plotted together with the HB stars in M13 (filled triangles), for comparison.

generated by the saturation of the color index as it becomes insensitive to changes in the temperature.

RC85 defined a X_{HB} coordinate which measured the star position along the HB as its projection on the theoretical ZAHB (see Figure 1 in RC85). Analogously Ferraro et al. (1992a,b), Dixon et al. (1996), and, more recently Catelan et al. (1997) have used a coordinate ℓ_{HB} , based only on observable quantities. ℓ_{HB} utilizes the mean ridge line for the linear coordinate along the HB in the observational plane. We will use ℓ_{HB} to study the peculiar distribution along the HB tail for the M13, M80 pair in more detail.

Because of the high degree of similarity of the main branches in M13 and M80 (see Fig 2), as first step we have selected the non-evolved HB stars in the $(V, U - V)$ plane in the co-aligned sample. A total sample of 492 stars (221 in M13 and 271 in M80) has been fit by a 6th order polynomial to define the mean ridge line. Each star was then projected onto the ridge line, and a curvilinear coordinate (ℓ_{HB}) has been computed along it. The zero point of the ℓ_{HB} coordinate has been arbitrarily taken to be $(U - V) = 1$.

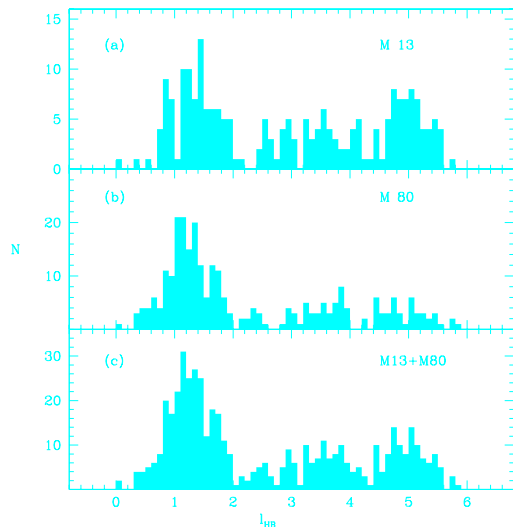


Fig. 6.— Histograms showing the ℓ_{HB} distribution for M13 [panel (a)], M80 [panel (b)] and for the co-added sample (M13 + M80); [panel (c)]. The zero point of the ℓ_{HB} coordinate has been assumed at $(U - V) = 1$, so low values of ℓ_{HB} correspond to the red side of the HB, high values to the extreme blue tail.

The ℓ_{HB} distributions for each cluster and the co-added sample are shown in Figure 6. From the inspection of panels (a) and (b) in Figure 6, it is evident that the stellar distribution along the tail of these clusters is quite complex. Despite the fact that neither HB is uniformly populated and the HB distribution is quite different in the two clusters, there are some striking similarities in their overall morphology. These similarities are generally best seen in the co-added sample displayed in panel (c). Note in particular:

1. The global length of the two HBs is approximately the same ($\ell_{\text{HB}} \sim 6$); only one star in M80 (located at $U - V = -1.8$) has been found beyond this limit.
2. The bulk of the reddest stars ends at the same location $\ell_{\text{HB}} \sim 2$.
3. The bluest groups start at the same location $\ell_{\text{HB}} \sim 4.4$.
4. The co-added sample shows at least three main groups of stars that could be modeled individually by separate gaussian distributions with different means and dispersions. These groups are

separated by two underpopulated regions (at $\ell_{\text{HB}} \sim 2.1$ and $\ell_{\text{HB}} \sim 4.3$). Additional “depressions” in the star counts are located at $\ell_{\text{HB}} \sim 2.7$ and $\ell_{\text{HB}} \sim 3.2$.

In the following we denote the three main groups of stars as follows:

UBT Upper blue tail HB stars: $\ell_{\text{HB}} < 2.1$

MBT Mid-blue tail HB stars: $2.1 < \ell_{\text{HB}} < 4.2$

LBT Lower blue tail HB stars $\ell_{\text{HB}} > 4.2$. It is the presence of a substantial population of LBT stars which sets EBT clusters apart from other BT clusters.

The relative population of the HB stars in these groups, and the values are given in Table 1. Interestingly, the fraction of stars in the LBT is much larger in M13 ($\sim 30\%$) than in M80 ($\sim 17\%$).

4.1. The gaps

Catelan et al. (1997) have recently discussed the problem of determining the statistical significance of the gaps. From an extensive set of the synthetic HBs they found that the procedure described by Hawarden (1971) and Newell (1973), often adopted to evaluate the significance of gaps (e.g., Ferraro & Paresce 1993, Crocker et al. 1988), substantially overestimates their statistical significance. As a first attempt to quantify the probability of finding gaps along the blue HB, they assumed that the stellar distribution in ℓ_{HB} coordinate is uniform, and computed the probability of a gap of given depth (number of stars in a given range of ℓ_{HB} less than some value) anywhere along the HB sequence. Under this idealized assumption the probability is naturally governed by the Binomial distribution

To follow their procedure we first plot in Figure 7 the normalized cumulative ℓ_{HB} distribution for M13 and M80. In this plot the gaps should appear as horizontal regions, and their location is indicated by arrows. The typical size of the gaps in this coordinate is $\delta\ell_{\text{HB}} \sim 0.4$, and the HB sequences has length up to $\ell_{\text{HB}} \sim 6$. Divide the BT into 15 bins of width $\delta\ell_{\text{HB}} \sim 0.4$. Given the total number of HB stars and the number of stars actually found in each gap, one can evaluate the probability that a gap of similar depth would be found somewhere along the blue HB.

TABLE 1
RELATIVE POPULATIONS OF STARS ALONG THE HB (SEE TEXT)

	UBT	MBT	LBT
M13	92	62	67
M80	169	57	45

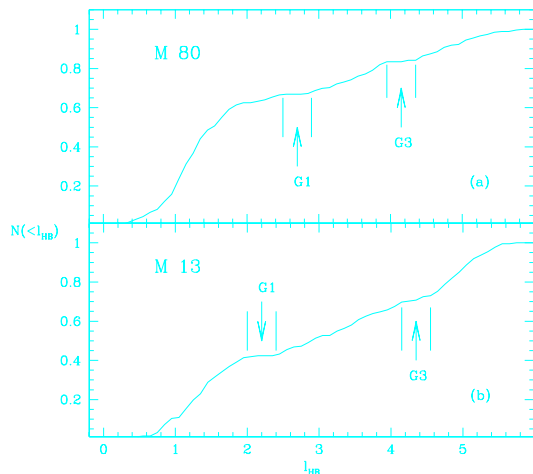


Fig. 7.— The l_{HB} cumulative distribution of the HB stars in M13 [panel (a)] and M80 [panel (b)]. Gap locations are indicated by arrows.

The bluest gap in M13 (G3) has quite a low statistical significance, with the probability that it is due to chance $\sim 20\%$. However, the probability that this depression in the star counts occurs *close to the same* l_{HB} value in both clusters remains small. All the other gaps that can be seen in the $(V, U - V)$ CMD, are deep enough to have quite high a statistical significance $(> 3.5\sigma)$.

5. Discussion

The variation of HB morphology among clusters of similar metallicity is known as the *second parameter* (2ndP) problem. However, all of the complexities of HB morphology may not be so easily classified. The 2ndP problem has aspects that require comment here

as a result of these new observations.

1. There is evidence in favor of a “global” 2ndP (Lee, Demarque and Zinn 1994, Fusi Pecci et al. 1993). By “global” we mean some process or circumstance that acts to vary HB morphology at fixed metallicity in the cluster system as a whole. We exclude from “global” individual differences between cluster HB morphology that might arise through exceptional circumstances in certain clusters (e.g., NGC 2808). One possible global 2ndP that has been explored extensively is age (Lee, Demarque and Zinn 1994, Chaboyer, Demarque, & Sarajedini 1996 and references therein), which shifts the peak of the HB color distribution to the blue.
2. Parameters that characterize the bulk HB morphology (Fusi Pecci et al. 1993) do not describe the overall extension of the BT. BTs may be driven by a special “2ndP,” which we will call the BT-2ndP. Fusi Pecci et al. (1993) and Buonanno et al. (1997) noted a strong correlation between the blue tail extension and the cluster central density, which they suggested as “a” 2ndP. Stellar rotation (Peterson, Rood, & Crocker 1995) and helium mixing (Sweigart 1997) are other plausible BT-2ndP. In addition, there is a subset of the BT clusters with highly extended blue tails (EBT clusters) in which mass loss goes to completion in a significant fraction of the HB stars. Until recently, NGC 6752 was the only known example of this morphology (Canon 1981), but in the last few years it has been joined by ω Cen (Whitney et al. 1994), NGC 2808 (Sosin et al. 1997), in addition to M13 and M80.
3. Features like the BT gaps may be regarded as 2ndP “fine structure.” Our tentative working assumption is that this fine structure is imposed

on the HB by RGB mass loss. Mass loss “structure” could well be linked to different physical processes like cluster core interactions or stellar rotation, or perhaps by other unknown factors—i.e., whatever is driving the BTs is also establishing the HB fine structure. The results of the processes causing these fine structure phenomena may look very different in clusters of higher and lower metallicity.

In Ferraro et al. (1997b), we made a comparison of the HB morphology of M3 and M13—an extreme example of a second parameter pair. Since the relative locations of the main loci (RGB, HB, MS-TO) of those clusters was quite similar, we argued that that *age cannot be responsible for the HB differences observed in M3 and M13*. Since the fiducial sequences of M13 and M80 can also be aligned, there is *no reason to infer that the age of M80 is significantly different from that of M3/M13*.

We can now bring M80 into the discussion to illuminate further the possible role of cluster dynamics on HB morphology. M3 and M13 have almost the same central density ($\log \rho_0 \sim 3.4 M_\odot \text{pc}^{-3}$) but different HB morphology (Ferraro et al. 1997b). M80 is one of the most concentrated clusters in the Galaxy ($\log \rho_0 \sim 5.3 M_\odot \text{pc}^{-3}$) which has no evidence for a core collapsed state (i.e. its surface brightness profile can be modeled by a King-Michie model). Despite the fact that M80’s core density is almost two orders of magnitude higher than that of M13, its HB morphology is very similar. Thus, either cluster density is not affecting HB structure in M13 & M80, or different BT-2ndP are at work in the clusters. Coupled with the fact that density cannot account for the M3/M13 difference, this appears to rule out density as the sole BT-2ndP.

Nevertheless, the correlation between BTs and high density seems very strong and cannot be discounted. Almost every high density cluster with $[\text{Fe}/\text{H}] \sim -1.5$ has a blue tail. Even some high metallicity, high density clusters (NGC 6388 and NGC 6441 Rich et al. 1997) have now been found to have the analog to a BT. In NGC 6388, for example, $\sim 16-20\%$ of the stars in core have suffered a large degree of mass loss. Yet 47 Tuc (O’Connell et al. 1997), which is almost as dense, has only a small number of blue HB stars, very few of which are in the core.

Beyond the observed correlation, an attraction of high cluster density as a BT-2ndP is that it is easy

to imagine that a multi-modal distribution blue stars might be produced through tidal interactions. One possibility was presented by Sosin et al. (1997) discussing the case of NGC 2808. They argue that the EBT with gaps in that cluster might arise through groups of stars undergoing events that strip discrete amounts of mass from RGB envelopes. The expectation would be that the most extreme mass loss happens to the stars with the highest number of interactions. A consequence of this mechanism is that the bluest stars would be relatively rare, which is not what is observed.

Likewise high density should be correlated with the number of capture-binaries (Bailyn et al. 1992). While binary evolution might account for sparsely populated BTs like the few stars in M3, or perhaps the few EHB stars beyond the bulk of the BT in M15, the substantial BTs we discuss here are almost certainly some variant of single HB stars. If they were not, neither population ratios (Buonanno, Corsi, & Fusi Pecci 1985) nor radial distributions (Ferraro et al. 1997b, Whitney et al. 1997) would be as observed. So while high density could plausibly produce BTs, no mechanism which fits the observations has yet been suggested.

Does the correlation of high density with BTs coupled with the fact that some low density clusters have BTs require that there are multiple BT-2ndPs? A single mechanism might suffice if high cluster density could produce BTs through some intermediary process. Let us suppose that process- \mathcal{BT} causes BTs. If high density cores could lead to process- \mathcal{BT} , perhaps via tidal interactions in the cluster core, this would explain the correlation between density and BTs. If process- \mathcal{BT} could also arise for other reasons, perhaps as a cluster initial condition, this would explain low density clusters with BTs.

As for 2ndP fine structure, we have argued that most of the gaps are statistically significant. Further, we have found that two (G1 and G3) or maybe even three (G0, G1 and G3) gaps are located at nearly the same temperature (within 1500 K) in M13 and M80. This evidence strongly suggests that some genuine physical mechanism produces the gaps. If a second parameter candidate could be shown to produce such features, it would be an important step toward resolution of this long-standing problem.

5.1. Gaps in other Clusters

Gaps in other BTHB clusters have been known for some time. How do these gaps compare to ours? Catelan et al. (1997) list 14 GCs that show gaps along the HB. Here we limit our discussion to BT gaps, excluding clusters which only show mid-HB (= near the RR Lyrae strip) gaps. Even in many BT clusters no explicit determination of the temperature at which each gap occurs has yet been made. Because of the difficulty of determining T_{eff} from B , V photometry alone, we will further restrict our discussion to clusters with available large sample UV photometry. These include

1. M79 (Hill et al. 1996)—Based on their UIT1 m_{152} , $m_{152} - m_{249}$ CMD we find a gap at 9900 K. A gap is seen at the same temperature in the ground based V , $B - V$ CMD of Ferraro et al. (1992a), There are only a few stars hotter than 20,000 K.
2. NGC 6681 (Watson et al. 1994)—Catelan et al. (1997) also note that the m_{160} , $m_{160} - V$ *HST* based CMD shows a gap at 8,700 K (see Figure 2 in Watson et al. 1994), which is nearly at the same temperature as G0. Moreover the clump of HB stars seems to have a break at 11,000 K, corresponding to the temperature of G1. There are only a few stars hotter than 18,000 K and the hottest star is at 22,000 K.
3. NGC 6752 (Landsman et al. 1996)—In a m_{162} , $m_{162} - V$ CMD based on UIT2 data there is a gap at 18,000 K.
4. M15 (Ferraro and Paresce 1993)—Based on ultraviolet HST-FOC observations, there is a gap at ~ 9000 K (again nearly at the same temperature as G0). The HB terminates at $\sim 15,500$ K. Metallicity is lower: $[\text{Fe}/\text{H}] = -2.15$ (Zinn 1985)
5. NGC 2808 (Sosin et al. 1997)—There are gaps at 25,000 K and 17,000 K (recall that the hottest gaps in M13 and M80 are at 18,000 K and 19,500 K respectively). The Zinn 1985 metallicity is somewhat higher: $[\text{Fe}/\text{H}] = -1.37$, but similar and within the uncertainties of abundance determinations.
6. ω Cen (Whitney et al. 1994)—In a m_{162} , $m_{162} - u$ CMD based on UIT1 data there is a gap at

16,000 K. Interpretation of ω Cen is complicated because of the spread in metallicity among the stars and because of the unexplained depression in UV luminosity of the hottest stars in the cluster (Whitney et al. 1997). The presence of a gap does suggest that whatever mechanism produces the ω Cen gap may also produces a gap at similar T_{eff} independent of metallicity.

Except as noted metallicities are all close to $[\text{Fe}/\text{H}] = -1.5$. These results are summarized in Table 2. A “Not EBT” entry denotes that the extended part of the BT is not substantially populated.

Identifying trends in such a compilation is difficult because: 1) There is “noise” in the gap data. Catelan et al. argue that gaps at random locations along the BT are not terribly unlikely. Hence we may be confused by a few statistical fluctuation gaps mixed in among “real” gaps. For example, G2 in M80 (but see below) and G3 in NGC 2808 might fall into this class since they have no counterparts in other clusters. 2) The data for different clusters is not very homogeneous. 3) Gaps cannot be located with high precision. Nevertheless, some conclusions that emerge are:

1. All clusters with EBTs have a at least one gap on the lower BT.
2. If one allows for some imprecision in the ω Cen results there is a suggestion that all EBT clusters have a gap (G3 in M13, M80, NGC 6752, and G2 in NGC 2808) at $\sim 18,000$ K. We will call this the 18kK gap.
3. G0 & G1 occur in many but not all clusters. The location and widths of these gaps may vary cluster to cluster, but are at similar locations in the clusters in which they are present.

5.2. Blue Tails and Gaps: A Naive Working Scenario

HB/post-HB evolutionary tracks change morphology at a T_{eff} similar to that of G3. The hotter stars (so-called extreme-HB or EHB) evolve essentially vertically in the H-R diagram and do not return to the asymptotic giant branch (AGB) after core He exhaustion. The entire post-HB evolution is spent at high T_{eff} as AGB-manqué stars (Dorman, Rood, & O’Connell 1993, Greggio & Renzini 1990). The cooler stars return to the AGB. It is tempting to identify the “18kK” gap with the onset of EHB behavior (Newell

TABLE 2
TEMPERATURE OF GAPS IN DIFFERENT CLUSTERS

	G0	G1	G2	G3
M13	9500K	11,000K		19,000K
M80	9500K	11,000K	12,000K	18,000K
NGC 6681	8700K	11,000K (?)		Not EBT
M79	9900K			Not EBT
NGC 6752				18,000K
M15	9000K			Not EBT
NGC 2808			17,000K	25,000K
ω Cen				16,000K

1973). Rood et al. (1997a,b) show that the transition from normal HB track morphology to EHB morphology does not produce a gap. However, a combination of this factor plus considering mass loss to be function of a random (but unimodal) mass loss efficiency (η_{ML}) as suggested by D’Cruz et al. (1996) can produce a gap (Whitney et al. 1997). Basically, a large range in η_{ML} produces EHB stars and thus a pile-up on the hot end of the HB. Coupled with a sparse population along the rest of the BT, this can lead to gap near but not necessarily at the normal-HB-EHB transition. While the D’Cruz et al. (1996) result was based on a specific model, they argued that the result was more general and that the distribution of stars below the EHB gap could lead to observational evidence as to how the RGB mass loss turns-off (Rood et al. 1997a).

The gap we have labeled G0 occurs frequently enough that it may be real. It occurs near the hot end of the traditional “horizontal” (in the V , $B - V$ CMD) HB.⁷ This gap is present in some but not all clusters.

The gaps G1 and G2 are more complicated because G2 appears in M80 but not M13. We suggest the following scenario (Refer to all three panels of Figure 5 for the following discussion.) Our working hypothesis is that BT-gaps arise because RGB mass loss does not uniformly populate the ZAHB. It seems unlikely that a mass loss process would produce a ZAHB region completely devoid of stars, and more likely that

there would be a mass loss range with low probability. This would produce a sparsely populated region of the ZAHB, which in combination with small number statistics could produce a gap. We suggest that the entire G1–G2 region is a “sparse population gap” (recall that the M80 stars in this region are slightly overluminous with respect to the cooler stars). Such a gap might contain a few near ZAHB stars. In addition, it might contain stars which originated from the more richly populated regions on the hot side of the gap that are now evolving back toward the AGB. The latter are analogous to the RR Lyrae population in clusters like M92 and would be more luminous than the bulk of the HB stars. (This group would not be present in G3 assuming our identification of G3 as the EHB gap is correct.) As luck would have it most of the G1–G2 stars in M13 are from the sparse ZAHB group, and those in M80 have evolved from the hotter parts of the HB.

No explanation for the G0 and G1/G2 leaps forward. One possibility is that there are two mass loss mechanisms, ML1 and ML2, driven by different engines. In all clusters mechanism 1 operates and produces a mean mass loss of $\sim 0.2 M_{\odot}$. ML1 almost certainly is a function of metallicity. For example, Fusi Pecci et al. (1993) argue that very metal-poor stars probably lose less total mass. In clusters where ML1 is the predominant mass loss mechanism, one observes normal 1stP behavior. In addition, a global 2ndP like age would produce the expected behavior, e.g., increasing age \Rightarrow bluer HB.

A second mechanism operates to different degrees in different clusters and on individual stars within

⁷Just as many white dwarfs are not white, we now know that many HBs are not horizontal. In this context we are drawn to the usage horizontal horizontal branch.

each cluster. In some clusters it is insignificant compared to ML1. Where it is significant, ML2 is basically the BT-2ndP. ML2 is probably driven by different engines including cluster density and stellar rotation. It may be accompanied by subsidiary effects like He-mixing which lead to diverse outcomes. If ML2 operates very efficiently, some HB stars are effectively removed from the distribution of ML1-only HB stars producing a gap. If ML2 is only mild, the ML1 + ML2 stars might form a tail merging into the ML1-only HB. This might fit the bimodality-without-a-gap suggested by Crocker et al. (1988) for clusters like M92.

Whether an alternate mechanism could mimic ML2 without additional mass is not clear. In the Sweigart (1997) He-mixing models, substantial mixing was usually accompanied by substantial mass loss, although the free-parameter space is large enough that this might not be required. In general though, it is easier to modify the composition of a RGB envelope if most of the envelope has been lost.

Clearly, building a case for a scenario like that above will require data from more clusters and a more precise determination of the gap parameters in each cluster. Also requiring further study is the nature of the gaps. Are there forbidden zones which should be completely devoid of stars except those scattered in by observational error? Perhaps as suggested above, they are just underpopulated regions?

5.3. Other Related Factors

There are other cluster phenomena which may be related to HB morphology. Even if a causal connection cannot be established it is worth searching for correlations.

The phenomenon most likely correlated with BTs is RGB mixing as shown through the abundances of the CNO elements. Catelan & de Freitas Pacheco (1995) noted the difference in RGB CNO processing in their study of M3 & M13. They searched for similar correlations in other clusters. In particular they note that the most highly processed super-oxygen-poor stars (SOP) of Kraft et al. (1992) are found only in clusters with very blue HBs. As far as we are aware, the required abundance study of M80 has not been done. We might predict on the basis of HB morphology that M80 will have SOP stars.

Norris (1983) noted a possible correlation between HB-morphology and cluster ellipticity. For the M3/M13

pair this seemed an interesting possibility (Ferraro et al. 1997b). For M80 the ellipticity is 0.06, compared to 0.01 & 0.12 for M3 & M13, respectively. So the correlation is neither strengthened nor weakened since M80 could be inclined to our line of sight.

Another perhaps remote possibility is a correlation with the parameters of the clusters' orbits in the Galaxy (e.g., Dauphole et al. 1996). The current sample of cluster orbits is small and does not include M80.

6. Summary

Using *HST* UV/visual observations we have found that the HB of the globular cluster M80 has a long blue tail extending below the MS-TO. The stellar distribution along the HB is not uniform, but contains four gaps. M80's HB is strikingly similar to that which we have found earlier in M13. In particular, the locations of three of the gaps are similar. Because of this we argue that the gaps are real, i.e., they are not statistical fluctuations, and that the gaps owe their origin to some yet unidentified physical process—most probably associated with RGB mass loss.

The role of central density in determining the HB morphology of M80, M3, and M13 is not at all simple. M13 and M3 have similar (lowish) densities and very different HBs. The density of M80 is almost two orders of magnitude higher and its HB morphology is quite similar to that of M13. The correlation of density and HB-BTs in other clusters is quite strong. We present a tentative working scenario: first, the 2ndP problem is perhaps not a single game (e.g., cricket and baseball—similar sports which are indistinguishable and incomprehensible to non-aficionados); second, there many players participating in the 2ndP games, to different degrees from cluster-to-cluster and star-to-star. Though this may seem to be *ad hoc*, we note that nature is complex and that these stars have lived crowded together for billions and billions of years.

RTR & BD are supported in part by NASA Long Term Space Astrophysics Grant NAGW-2596 and STScI/NASA Grant GO-5903. The financial support by the *Agenzia Spaziale Italiana* (ASI) is gratefully acknowledged.

REFERENCES

- Bailyn, C. D., Sarajedini, A., Cohn, H., Lugger, P. M., & Grindlay, J. E. 1992, *AJ*, 103, 1564
- Borissova, J., Catelan, M., Spassova, N., & Sweigart, A. V. 1997, *AJ*, 113, 692
- Brocato, E. et al. 1997, in preparation
- Buonanno, R., Corsi, C., and Fusi Pecci, F. 1985, *A&A*, 145, 97
- Buonanno, R., Caloi, V., Castellani, V., Corsi, C. E., Fusi Pecci, F., & Gratton, R. 1986, *A&AS*, 66, 79
- Buonanno, R., Corsi, C. E., Bellazzini, M., Ferraro, F., & Fusi Pecci, F. 1997, *AJ*, 113, 706
- Cannon, R. D. 1981 in *Astrophysical Parameters for Globular Clusters*, ed. A. G. D. Philip, (Schenectady: L. Davis), 501
- Carretta, E. & Gratton, R. G. 1997, *A&AS*, 121, 95
- Catelan, M., & de Freitas Pacheco, J. A. 1995, *A&A*, 297, 345
- Catelan, M., Borissova, J., Sweigart, A. V., & Spassova, N., 1997, *ApJ*, submitted
- Chaboyer, B., Demarque, P., & Sarajedini, A. 1996, *ApJ*, 459, 558
- Crocker, D. A., Rood, R. T. & O'Connell, R. W. 1988, *ApJ*, 332, 236
- Dauphole, B., Geffert, M., Colin, J., Ducourant, C., Odenkirchen, M., Tucholke, H.-J. 1996, *A&A*, 313, 119
- D'Cruz, N. L., Dorman, B., Rood, R. T., O'Connell, R. W. 1996, *ApJ*, 466, 359
- de Boer, K. S. 1995, *A&A*, 142, 321
- Dixon, W. V. D., Davidsen, A. F., Dorman, B., Ferguson, H. C. 1996, *AJ*, 111, 1936
- Dorman, B., Rood, R. T., & O'Connell, R. W. 1993, *ApJ* 419, 596
- Dorman, B. et al. 1997a, *ApJ*, 480, L31
- Dorman, B., Paltrinieri, B., Ferraro, F. R., Fusi Pecci, F., & Rood, R. T., 1997b, *AJ*, submitted
- Ferraro, F. R., Clementini, G., Fusi Pecci, F., Buonanno, R., & Alcaïno, G. 1990, *A&AS*, 84, 59
- Ferraro, F. R., Clementini, G., Fusi Pecci, F., Sortino, R., Buonanno, R. 1992a, *MNRAS*, 256, 391
- Ferraro, F.R., Clementini, G., Fusi Pecci, F., Vitiello, E., Buonanno, R. 1992b, *MNRAS*, 264, 273
- Ferraro, F. R., Paltrinieri, B., Fusi Pecci, F., Cacciari, C., Dorman, B., Rood, R. T., Buonanno, R., Corsi, C. E., Burgarella, D., Laget, M. 1997a, *A&A*, in press
- Ferraro, F. R., Paltrinieri, B., Fusi Pecci, F., Cacciari, C., Dorman, B., & Rood, R. T. 1997b, *ApJ*, 484, L145
- Ferraro, F. R., & Paresce, F. 1993, *AJ*, 106, 154
- Fusi Pecci, F., & Renzini, A. 1978, in *IAU Symposium No. 80, The HR Diagram*, ed. A. G. D. Philip & D. S. Hayes (Dordrecht: Reidel), 225
- Fusi Pecci, F., Ferraro, F. R., Bellazzini, M., Djorgovski, D.S., Piotto, G., Buonanno, R., 1993, *AJ*, 105, 1145
- Fusi Pecci, F. 1996, in *Formation of the Galactic Halo, Inside and Out* eds. H. Morrison & A. Sarajedini (San Francisco: ASP), 221
- Greggio, L. & Renzini, A., 1990, *ApJ*, 364, 35
- Hawarden, T. G. 1971, *Observatory*, 91, 78

Hill, R. S. et al. 1996, AJ, 112, 601

Holtzmann, J. A., Burrows, C. J., Casertano, S., Hester, J. J., Trauger, J. T., Watson, A. M., Worthey, G., 1995, PASP, 107, 1065

Kraft, R. P., Sneden, C., Langer, G. E., & Prosser, C. F. 1992, AJ, 104, 645

Landsman, W. B., et al. 1996, ApJ, 472, 93

Lee, Y-W., Demarque, P., and Zinn, R. J. 1994, ApJ, 423, 248

Newell, E. B. 1973, ApJS, 26, 37

Norris, J. 1983, ApJ, 272, 245

O'Connell, R. W., Dorman, B., Shah, R. Y., Rood, R. T., Landsman, W. B., Bohlin, R. C., Neff, S. G., Roberts, M. S., Smith, A. M., & Stecher, T. P. 1997, AJ, in press

Peterson, R. C., Rood, R. T., Crocker, D. A. 1995, ApJ, 453, 214

Renzini, A. 1977, in *Advanced Stages of Stellar Evolution*, ed. Bouvier & A. Maeder (Geneva: Geneva Obs.), 151

Rich, R. M., et al. 1997, ApJ, July 20

Rood, R. T. & Crocker, D. A. in *Horizontal Branch and UV-Bright Stars 1985*, ed. A. G. D. Philip (Schenectady: L. Davis), 99

Rood, R. T. 1997, in *Fundamental Stellar Properties: The Interaction Between Theory and Observation*, eds. T. R. Bedding, A. J. Booth, & J. Davis (Dordrecht: Kluwer), 363

Rood, R. T., Whitney, J.H., D'Cruz, N. in *Advances in Stellar Evolution 1997*, eds. R. T. Rood and A. Renzini, (Cambridge Contemporary Astrophysics), 74

Shara M. M., Drissen L., 1995, ApJ, 448, 203

Sosin, C., et al. 1997, ApJ, 480, L35

Sweigart, A. V. 1997, ApJ, 474, L23

Stetson, P. B., Vandenberg, D. A., Bolte, M., 1996, PASP, 108, 560

Walker, A. R. 1992, PASP, 104, 1063

Watson, A. M., et al. 1994, ApJ, 435, 55

Whitney, J. H., et al. 1994, AJ, 108, 1350

Whitney, J. H., et al. 1997, submitted to AJ.

van Albada, T. S., de Boer, K. S., & Dickens, R. J. 1981, MNRAS, 195, 591

Zinn, R. J. 1985, ApJ, 293, 424